INTENSE BEAM ISSUES IN CSNS ACCELERATOR BEAM COMMISSIONING

L. Huang[1], M. Huang[1], S. Xu[1], H. Liu[1], L. Rao[1], X. Lu[1],
Y. Li[1], J. Chen[1], Y. An[1], Z. Li[1], J. Peng[1], X. Luo[1], S. Wang[†,1]
Institute of High Energy Physics, Chinese Academy of Sciences, Beijing, China
[1]also at Spallation Neutron Source Science Center, Dongguan, China

Abstract

The China Spallation Neutron Source (CSNS) consists of an 80 MeV H⁻ Linac, an 1.6 GeV Rapid Cycling Synchrotron (RCS), beam transport lines, a target station, and three spectrometers. The CSNS design beam power is 100 kW, with the capability of upgrading to 500 kW. In August 2018, the CSNS was officially opened to domestic and international users. By February 2020, the beam power had reached 100 kW. With the implementation of improvements such as the addition of harmonic cavities, the beam power was further increased to 140 kW in Oct. 2022. During the beam commissioning, the most significant factor limiting the beam power was the beam loss caused by space charge effects and collective instabilities. The unexpected collective effects, the coherent oscillation of the bunches, were observed when the beam power exceeded 50 kW. By implementing the various mitigations, the beam loss caused by space charge effects and collective instabilities were effectively controlled. This paper is focused on these intense beam issues observed during the beam commissioning and the methods utilized to mitigate them. Additionally, the study on the collective effects in the upgrade project (CSNS-II) is also introduced.

INTRODUCTION

The China Spallation Neutron Source (CSNS) [1, 2] comprises of an 80 MeV H⁻ Linac, a 1.6 GeV Rapid Cycling Synchrotron (RCS), beam transport lines, a target station, and three spectrometers. The RCS accumulates 80 MeV beam through a multi-turn charge-exchange scheme and accelerates the beam to 1.6 GeV with repetition rate of 25 Hz. The RCS provides beam power of 100 kW with intensity of 1.56×10^{13}. In the upgrade of CSNS (CSNS-II), the beam power will be upgraded to 500 kW with an injection energy of 300 MeV. Due to the high beam intensity and high repetition rate, the beam loss must be controlled to a much lower level.

The RCS is a four-fold structure. Each super-period consists of two straight sections and an arc section. There are four 11-meter uninterrupted straight sections, and this benefits for accommodation of injection, extraction, RF cavity and transverse collimation system. Figure 1 displays the Twiss parameters in one super-period, and the main parameters of CSNS and CSNS-II are respectively listed in Table 1. The lattice is based on triplet cells with circumference of 227.92 meters, including 24 dipole

magnets and 48 quadrupole magnets, all excited by a 25 Hz DC-biased sinusoidal current pattern [3]. The 48 quadrupoles are powered by 5 families power supply. The nominal tune is set as (4.86, 4.78) with natural chromaticity of (-4, -9). Although the chromaticity correction is not mandatory for the RCS running below transition energy, the DC sextupole is applied for a better control over the chromaticity. The focusing and defocusing sextupole magnets, eight magnets in each family are powered by one power supply, are accommodated in the arc where the horizontal dispersion is about 2 meters, and the chromaticity is corrected to reduce the tune spread, specially at low beam energy stage. Due to that the DC field of sextupole magnet is not ramped with the beam energy, the chromaticity will decrease with the energy increasing. The transverse acceptance of the RCS is designed as 540 π·mm·mrad.
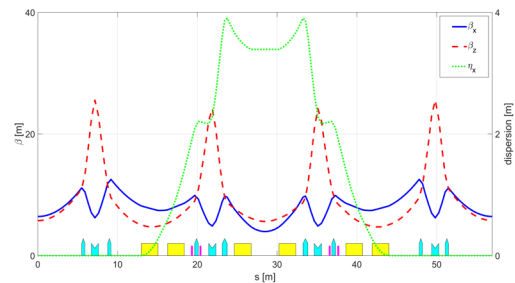
Figure 1: The Twiss parameters of RCS.

Table 1: Main RCS Parameters

Parameter	Unit	CSNS	CSNS-II
Circumference	m	227.92	227.92
Energy (Inj./Ext.)	GeV	0.08/1.6	0.3/1.6
Repetition rate	Hz	25	25
Bunch number		2	2
Beam intensity	10^{13}	1.56	7.8
Nominal tune (H/V)		4.86/4.78	4.86/4.78
Chromaticity (H/V)		-4/-9	-4/-9
SC tune shift		0.27	0.17
RF Voltage	kV	165	170

The RF acceleration system consists of eight ferrite loaded cavities [4]. The designed frequency and voltage pattern are shown in Fig. 2. In order to ensure the maximum efficiency in the process of beam capture,

wangs@ihep.ac.cn

accumulation and acceleration, the voltage gradually increases to carefully shrink the bucket size. The maximum cavity voltage is 165 kV with a maximum synchronous phase of 45 degrees. A dual harmonic RF system [5] will be implemented to increase the bunching factor in order to mitigate the space charge effects. One magnetic alloy (MA) cavity [6] has been installed in the tunnel, and a total of three cavities will be installed.
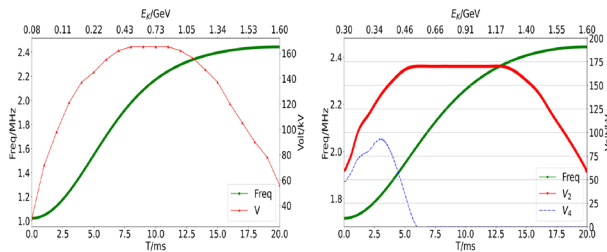
Figure 2: RF frequency and voltage pattern in the RCS of CSNS (left) and CSNS-II (right).

OVERVIEW OF BEAM COMMISSIONING

Figure 3 displays the beam power upgrading process of CSNS. The commissioning of the linac beam commenced in April 2017 [7], followed by the RCS commissioning in May 2017. Subsequently, on July 7, 2017, the beam was successfully accelerated to 1.6 GeV. Firstly, we conducted corrections for closed orbit distortion, lattice calibration, and matching among the dipole field, injected beam energy and RF frequency during the acceleration process [8]. The entire commissioning process followed a gradual power increase approach. After reaching each intermediate target, a relatively long-term stable operation has been carried out. Coherent oscillation has been observed firstly when the beam power achieved 50 kW, but it is easily tamed, and the beam power was increased to 50 kW with low beam loss level in January 2019 [9]. Subsequently, the limitation in realizing higher beam intensity was large beam loss induced by space charge (SC) and beam instability [10]. The bunching factor [11] and transverse painting injection [12] were optimized to uniform beam and reduce the space charge induced beam loss. The tune pattern in a typical acceleration cycle was also optimized based on the space charge tune shift and beam instability [13]. By adjusting the polarity of the DC sextupole to the opposite direction, the chromaticity was effectively optimized to suppress the beam instability. Through the implementation of various optimization techniques such as adjusting the bunching factor, injection painting, tune tracking pattern, and chromaticity, the beam commissioning was successfully concluded in February, 2020, reaching the designed beam power of 100 kW.

Following the completion of the beam commissioning, efforts were made to further enhance the power of the CSNS. In the summer of 2021, the DC sextupole magnets were replaced with AC ones, along with their corresponding power supply. The AC sextupole field has been implemented after the summer to improve the RCS transmission and suppress the instability simultaneously.

Furthermore, sixteen trim quadrupole magnets (QT) were installed during the same period. The combined utilization of AC sextupole and QT contributed to an increase in beam power to 125 kW. In the summer of 2022, the installation of the first MA cavity aimed to enhance the uniformity of the beam distribution in the longitudinal plane and mitigate the space charge effects. This upgrade resulted in the successful attainment of a beam power of 140 kW, while maintaining acceptable levels of beam loss. As of now, the CSNS is operating for users with a beam power of 140 kW.
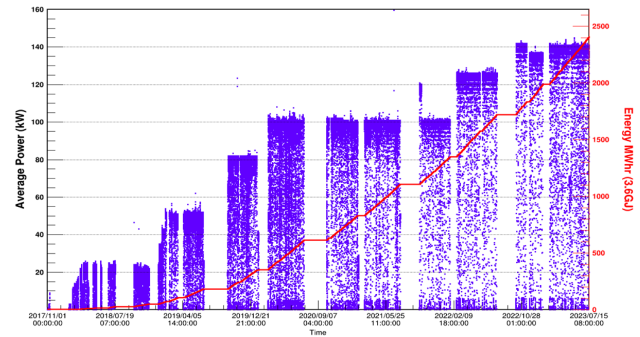
Figure 3: Beam power ramp-up history of CSNS, where the blue bars correspond to the beam power and the red line shows the accumulated beam power.

SPACE CHARGE EFFECTS

The space charge effects are a key problem for the high intensity proton accelerators, which directly affects the beam injection process and accumulation [14, 15]. Its effects mainly include: affecting the transverse and longitudinal beam focusing, causing the beam collective instability. Figure 4 shows the influence of the space charge effects on the circulating beam distribution while the anti-correlated painting is used for the CSNS.
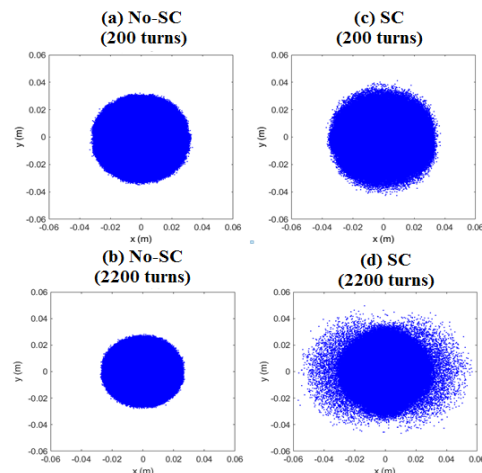
Figure 4: Influence of the space charge effects on the circulating beam distribution while the anti-correlated painting is used for the CSNS. "No-SC" and "SC" stand for ignoring and considering space charge effects, respectively. The turn number of the injection painting process is 200, and the first 2000 turns in the acceleration process.

MOA1I3

Transverse Space Charge Effects

For high intensity proton accelerators, in order to control the strong space charge effects, the phase space painting method is used for injecting a small emittance beam from the Linac into the large ring acceptance. The transverse phase space painting method can be divided into correlated painting and anti-correlated painting. For the CSNS, the anti-correlated painting scheme was adopted as the basic scheme for the injection system [16].

By using the anti-correlated painting, combined with other optimizations, the beam power of the CSNS accelerator has reached 50 kW and stable machine operation has been achieved [12]. However, in the higher beam power commissioning, an instability has been observed for the nominal tune, which produces a large amount of beam loss. To cure the instability, a tune tracking pattern [13], which the tune goes slowly down from the initial value of (4.80, 4.87), has been adopted. However, by using the new mode, a series of problems has been found with the anti-correlated painting, for instance, too large beam size after painting, non-uniform beam distribution, large transverse coupling caused by space charge effects.

Referring to the theoretical and machine study of J-PARC on the choice of the painting method, because of the effect of the space-charge coupling caused by the Montague resonance [17], when the betatron tunes are selected close to the coupling, the anti-correlated painting has more advantages for a large painting area and the correlated painting has more advantages for a small painting area. For instance, when a painting area is about 50 π·mm·mrad, compared to the anti-correlated painting, the beam distribution after the correlated painting is more uniform which leads to slower emittance growth. Therefore, for the optimized tune and maximum vertical painting area of about 75 π·mm·mrad in the RCS, the correlated painting may have more advantages than the anti-correlated painting design scheme.

In order to achieve the correlated painting, a new method to perform the correlated painting based on the mechanical structure of the anti-correlated painting scheme is proposed [18]. The method had been successfully applied to the RCS beam commissioning. Figure 5 shows the comparison of the transverse beam distributions for the correlated and anti-correlated painting measured in the beam commissioning. Compared to the case of anti-correlated painting, the transverse beam size for the correlated painting is smaller and the beam distribution is much better. Figure 6 shows the comparison of the transverse coupling caused by the space charge effects for the correlated and anti-correlated painting. Compared to the case of anti-correlated painting, the transverse coupling effect for the correlated painting in the vertical plane is relatively small. In addition, different from the anti-correlated painting, the correlated painting causes no significant changes in the horizontal beam distribution due to the variation of the vertical painting range. By using the correlated painting method, the difficulties encountered in

the high-power beam commissioning have been successfully solved.
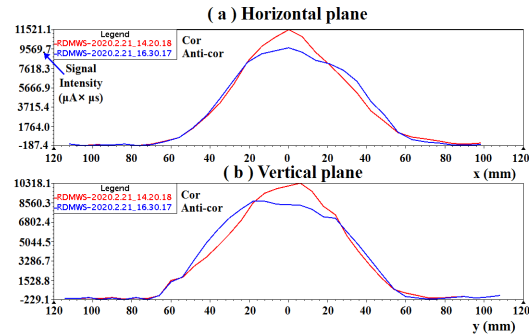
Figure 5: Comparison of the transverse beam distributions for the correlated and anti-correlated painting during the beam commissioning under the same conditions.
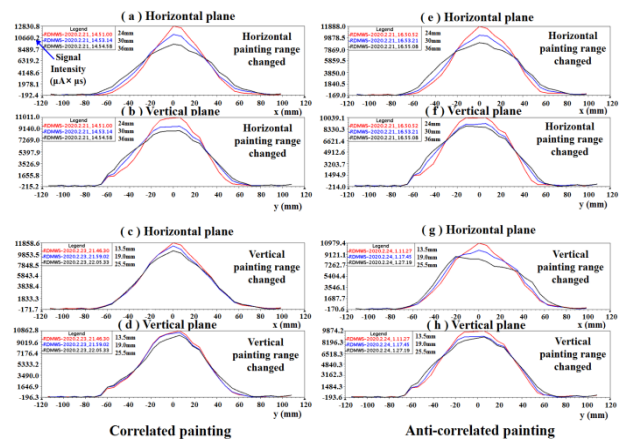
Figure 6: The transverse coupling caused by the space charge effects for the correlated and anti-correlated painting measured in the beam commissioning.

Longitudinal Space Charge Effects

A good way to mitigate the strong space charge effects is to uniform the longitudinal beam distribution, namely to improve the bunch factor. With only the fundamental cavity during the CSNS beam commissioning, we found that increasing the energy deviation between the injected beam and the synchronous particle of the RCS is very effective to obtain uniform beam in longitudinal plane. The optimization in detail is displayed in the reference [11].

By using dual harmonic RF cavity system to reduce the space charge effect is one of the main methods of power upgrade [19]. Specifically, the bunching factor can be increased to suppress the space charge tune shift. In the summer of 2022, a dual harmonic RF cavity system has been installed. By using the dual harmonic RF cavity system, the bunching factor was optimized and the longitudinal injection painting have been achieved. Figure 7 shows the optimization of the bunching factor. It can be found that the bunching factor has be increased after the optimization. Figure 8 shows the comparison of the longitudinal beam distributions with and without phase sweeping. By optimizing the longitudinal beam dynamics

in the RCS, combined with other optimizations, the beam power has been increased from 125 kW to 140 kW.
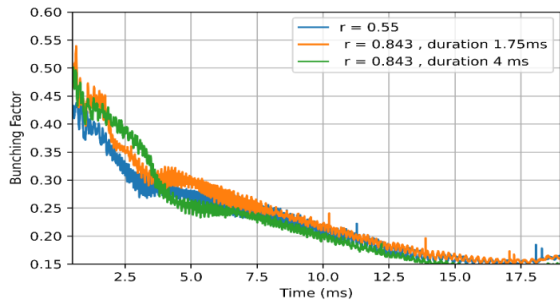
Figure 7: Optimization of the bunching factor. 'r' is the ratio of the second harmonic voltage to fundamental one.
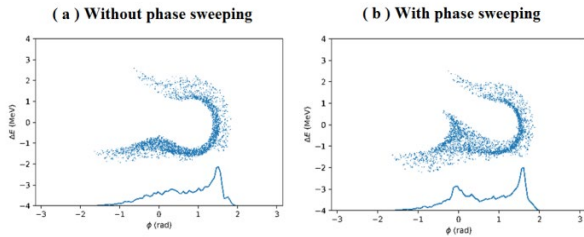
Figure 8: Comparison of the longitudinal beam distributions without and with phase sweeping.

OBSERVED BEAM INSTABILITY

Beam Instability Observation

A measurement campaign has been undertaken in detail to characterize the instability in a typical acceleration cycle. The Turn-by-Turn (TbT) beam position, growth rate of beam position and head-tail mode are the observables of interest. The result demonstrates that the observed instability is a head-tail type coupling bunch instability. Its dependence on the tune and chromaticity is illustrated below.

Several sets of measurement have been done for different tune in horizontal plane with natural chromaticity. The horizontal tune ν_x is changed from 4.78 to 4.86 while the vertical tune is kept constant as $\nu_y = 4.78$. The TbT beam position is shown in Fig. 9. Two buckets are perfectly filled and the total number of particles is 1.56×10^{13}, corresponding to a beam power of 100 kW. The oscillation happens, the oscillation amplitude increases rapidly as the tune moves toward 5.0 from below and the instability shows up later. The beam position is acquired by a beam position monitor located in injection area, and therefore the bump for injection painting before 0.4 ms can be clearly seen in the figure.

No specific instability mitigation strategy was planned in the RCS initial design. However, the implementation of a DC sextupole field provided a convenient means for mitigating the instability by increasing chromaticity in absolute value $|\xi|$ through polarity changes. The polarity of sextupole magnet was changed to cure the instability during the beam commissioning. In the presence of DC sextupole field, the chromaticity is different throughout the

acceleration cycle. For the sake of simplicity, a systematic measurement is carried out in the DC mode with constant energy of 80 MeV. Figure 10 gives the horizontal TbT beam position and survived particles with equivalent beam power of 45 kW. The legend in the figure is the chromaticity in transverse plane. In the measurement, the instability in vertical plane has not been observed and the vertical chromaticity is not constant for convenient adjusting that in horizontal plane.
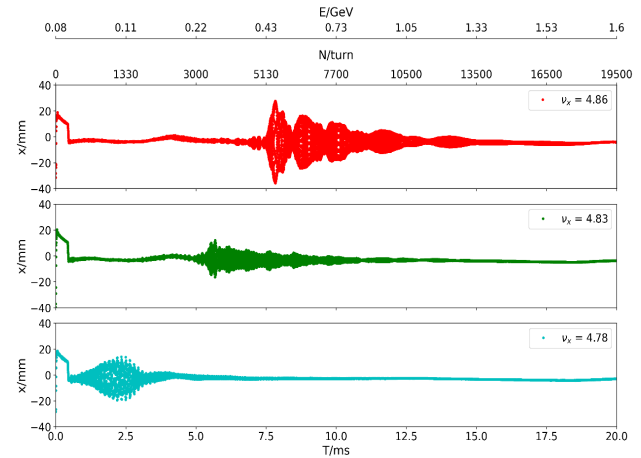
Figure 9: TbT beam position at different horizontal tunes with natural chromaticity.
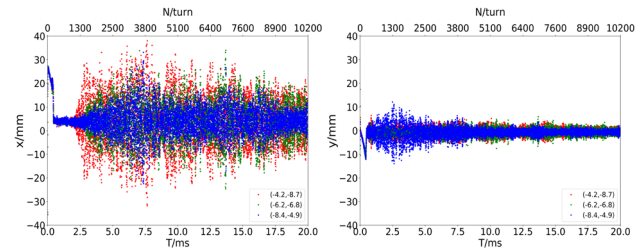
Figure 10: TbT beam position with different chromaticities in the DC mode.

Instability Mitigation

These measured results provide us a good guide to suppress the instability: optimization of the tune and the chromaticity. Considering that the space charge tune shift is about 0.27 at low energy stage, so the tune should be large at the beginning. As the space charge tune shift decreases with the energy ramping, the tune can decrease accordingly. Thus, a tune tracking pattern has been optimized to suppress the instability while keeping space charge effects under control at the same time. One of such a tune pattern for the operation mode is finally adopted [13]. The chromaticity in an acceleration cycle with DC power supplies is optimized after the tune optimization. The optimized chromaticity is (-9.8, -5.2) at injection and about (-9, -6.5) at ~2.5 ms. The TbT beam position and beam survival curve with three different modes are compared in Fig. 11 to realize the 100-kW beam power commissioning.

After reaching the designed beam power, two families of AC power supply have been adopted to have a flexible

control of the chromaticity and the chromaticity can be kept constant in the acceleration cycle. Beam experiment with AC sextupole field has been carried out immediately with beam power of 80 kW, where the horizontal chromaticity is set from -2 to -8 with the nominal tune settings. Figure 12 displays the horizontal beam position and beam survival curve, indicating that the instability is effectively suppressed when the chromaticity is below -8.
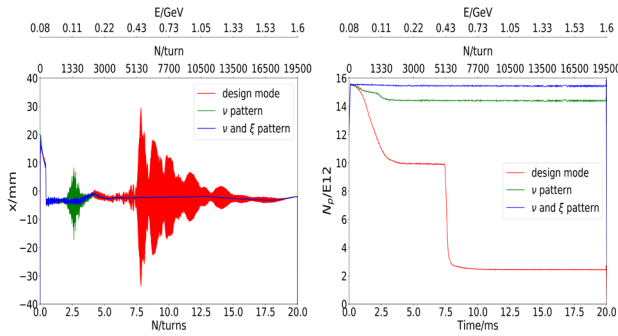
Figure 11: Measured TbT horizontal beam position (left) and the beam survival curve (right) in an RCS acceleration cycle for the design mode, the operation mode with tune optimization (tune pattern), and additionally with the chromaticity optimization with DC sextupole field.
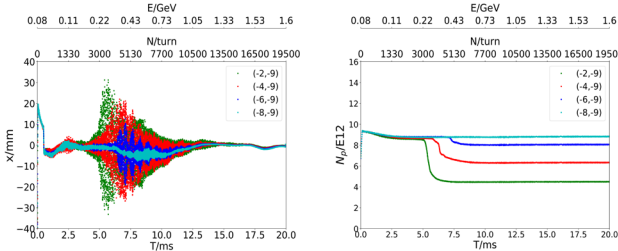
Figure 12: TbT measured beam position and the beam survivals curve for different consistant chromaticity.
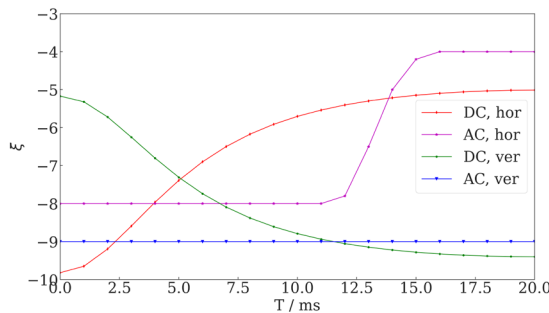
Figure 13: The chromaticity pattern with AC and DC sextupole field.

The beam behavior of the AC sextupole filed is compared with that of DC field in the operation mode. The optimized chromaticity with AC and DC field are shown in Fig. 13. The chromaticity of AC field is (-9, -9) before 11 ms and the sextupole field is quickly reduced to zero to big dynamic aperture. Figure 14 presents the beam position and RCS transmission obtained without sextupole, as well as with DC and AC sextupole, at a higher beam power of 125 kW. Obviously, with the AC sextupole field, the

amplitude of beam oscillation looks smaller and the RCS transmission is increased by about 2 %, which is vital importance for RCS operation.
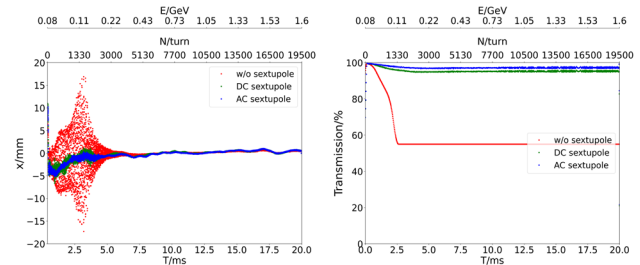
Figure 14: The horizontal TbT beam position (left) and RCS transmission (right) for operation mode without sextupole field and with optimized DC and AC sextupole field.

Possible Source

Impedance is a common instability source. However, it is difficult to identify the primary sources responsible for the observed instability based on the provided impedance model [20, 21]. The impedance has been re-investigated since the instability observed experimentally. The impedance of ceramic chamber has been calculated based on IW2D [22, 23], and the simulated impedance in Fig. 15 indicates that the ceramic chamber could potentially be the source.
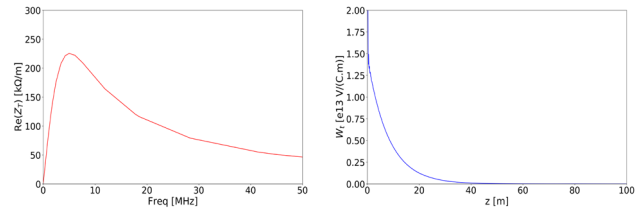
Figure 15: The real part of impedance (left) and wake (right) for the ceramic chamber, where the inner radius of the chamber is 120 mm with a length of 130 meters. The cross section of the chamber in the RCS is almost circular.

PROSPECTIVE APPROACHES TO MITIGATE THE INSTABILITY IN CSNS-II

The number of accumulated protons in CSNS-II is expected to increase by a factor of five. However, the main factors that limit the increase in beam intensity are the impedance induced beam effects. Specifically, an instability has been observed in CSNS, further highlighting the significance of these factors. The simulation study [24] was conducted using the RCS impedance mode and Fig. 16 illustrates the simulated result with beam power of 500 kW, the head-tail coupling bunch instability will appear and the threshold power is about 300 kW. In the simulation, the nominal tune is set and chromaticity optimization is also considered.

Adjusting the tune is an effective way to avoid the instability, and thus an experiment was conducted to compare the beam behavior for tunes above and below the integer value. Figure 17 presents measured result. The

beam power was scanned from 50 kW to 140 kW and no instability was observed in all cases with $\nu_x = 4.3$, making this mode highly promising for avoiding beam instability.

Landau damping is an effective method to suppress the beam instability [25], so simulations were also conducted using an octupole magnetic field in the operation mode at the beam power of 200 kW. Figure 18 illustrates the beam position in terms of different octupole strengths, demonstrating the effectiveness of the octupole field in mitigating RCS instability. Furthermore, the feedback system is also being planned.
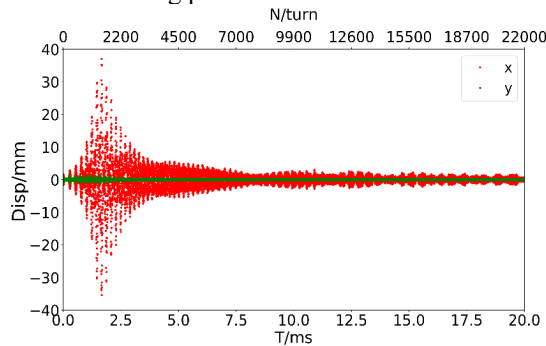
Figure 16: Prediction of the beam instability with 500 kW beam power in CSNS-II.
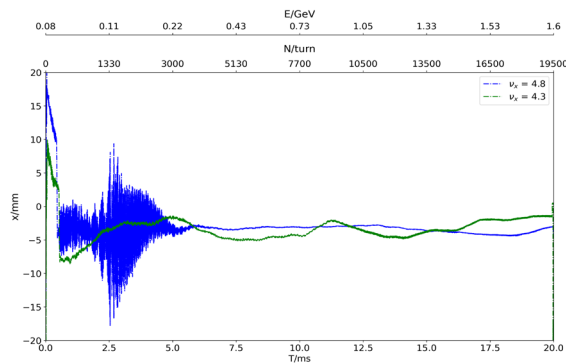
Figure 17: Measured beam position for tune with below and above integer with natural chromaticity. The vertical tune is 4.78 for $\nu_x = 4.8$ while it is 5.3 for $\nu_x = 4.3$.
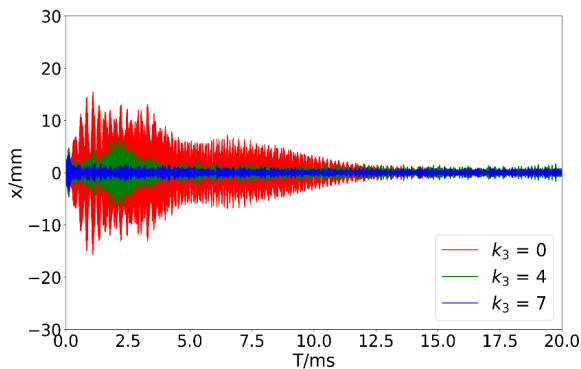
Figure 18: Simulated beam position in term of different octupole strength in the RCS of CSNS, where the optimized tune tracking pattern is used with natural chromaticity and the beam power is about 200 kW, corresponding to the proton number of 3.12×10^{13}.

SUMMARY

The high intensity issues played the most important role in the RCS beam commissioning in the CSNS. A series optimizations had been done to reduce the beam loss. The beam distribution at injection was optimized by employing techniques such as painting in the transverse plane and adjusting the bunching factor in the longitudinal plane. Different tunes were compared and optimized to enhance the beam transmission. A head-tail coupling bunch instability in transverse plane has been observed during the RCS beam commissioning. To mitigate this instability, optimization techniques including adjusting the tune tracking pattern and chromaticity with a DC sextupole field were implemented. These methods successfully suppressed the instability and contributed to the achievement of the designed beam power.

Furthermore, for the requirements to control tune spread and suppress the instability for accumulating higher beam intensity, the AC sextupole field replaced DC ones and the beam loss is further reduced. Additionally, one dual harmonic cavity was employed to mitigate the space charge effects. Those upgrades make the beam power reached 140 kW successfully and the beam loss were at acceptable level.

The bam power will be upgrade to 500 kW in the next few years, which will pose more challenges in the instability mitigation. More measurements and a thorough understanding of the instability need to be done. Novel methods of mitigation should be taken into consideration.

ACKNOWLEDGMENT

REFERENCES

[1] "China Spallation Neutron Source design report", Beijing: Institute of High Energy Physics, 2010.

[2] S. Wang *et al.*, "Introduction to the overall physics design of CSNS accelerators", *Chin. Phys. C,* vol. 33, no. S2, pp. 1-3, Jun. 2009. doi:10.1088/1674-1137/33/S2/001

[3] X. Qi, J. Zhang, Z. Hao., and W. Zhang, "Magnet power supply system for China Spallation Neutron Source", *Power Electron. Technol.,* vol. 48, no. 12, pp. 8-11, 2014 (in chinese). doi:10.3969/j.issn.1000-100X.2014.12.002

[4] X. Li *et al.*, "Design and progress of RF system for CSNS/RCS", *Atomic Energy Science and Technology,* vol. 50, no. 7, pp. 1307-1313, 2016. doi:10.7538/yzk.2016.50.07.1307

[5] H. Liu *et al.*, "Beam dynamics simulation about the dual harmonic system by PyORBIT", *in Proc. IPAC'21,*

Campinas, Brazil, May 2021, pp. 4194-4196.
doi:10.18429/JACoW-IPAC2021-THPAB207

[6] B, Wu, H. Sun, X. Li, C.-L. Zhang, and J.-Y. Zhu "Higher harmonic voltage analysis of magnetic-alloy cavity for CSNS/RCS upgrade project". *Radiat. Detect, Technol. Methods*, vol. 4, pp. 293–302, 2020.
doi:10.1007/s41605-020-00183-z

[7] J. Peng *et al.*, "Beam commissioning results of the CSNS Linac", *in Proc. IPAC'17*, Copenhagen, Denmark, May 2017. doi:10.18429/JACoW-IPAC2017-TUOBA1

[8] S. Wang, "Status of CSNS beam commissioning", presented at. HB'18, Daejeon, South Korea, Jun. 2018, paper MOA2PL01, unpublished.

[9] S. Xu *et al.*, "Beam commissioning experience of CSNS/RCS", *in Proc. IPAC'19*, Melbourne, Australia, May 2019, p. 1012–1014 .
doi:10.18429/JACoW-IPAC2019-MOPTS068

[10] L. Huang, S. Y. Xu, and S. Wang, "The characteristic of the beam position growth in CSNS/RCS", *in Proc. IPAC'21*, Campinas, SP, Brazil, May 2021.
doi:10.18429/JACoW-IPAC2021-TUPAB262

[11] L. Huang *et al.*, "Longitudinal dynamics study and optimization in the beam commissioning of the Rapid Cycling Synchrotron in the China Spallation Neutron Source", *Nucl. Instrum. Methods, Phys. Res., Sect. A*, vol. 998, p. 165204, 2021.
doi:10.1016/j.nima.2021.165204

[12] M. Huang *et. al.*, "Study on the anti-correlated painting injection scheme for the Rapid Cycling Synchrotron of the China Spallation Neutron Source", *Nucl. Instrum. Methods Phys. Res., Sect. A*, vol. 1007, p. 165408, 2021.
doi:10.1016/j.nima.2021.165408

[13] S. Xu *et al.*, "Beam commissioning and beam loss control for CSNS accelerators", *J. Instrum.*, vol. 15, no. 7, p. 07023, Jul. 2020. doi:10.1088/1748-0221/15/07/P07023

[14] J. A. Holmes, V. V. Danilov, J. D. Galambos, D. Jeon, and D. K. Olsen, "Space charge dynamics in high intensity rings", *Phys. Rev. Spec. Top. Accel. Beams,* vol. 2, p. 114202, 1999. doi:10.1103/PhysRevSTAB.2.114202

[15] S. Xu and S. Wang, "Study on space charge effects of the CSNS/RCS", *Chin. Phys. C,* vol. 35, p. 1152, 2011.
doi:10.1088/1674-1137/35/12/014

[16] M.-Y. Huang, S. Wang, J. Qiu, N. Wang, and S.-Y. Xu, "Effects of injection beam parameters and foil scattering for CSNS/RCS", *Chin. Phys. C,* vol. 37, no. 6, p.~067001, 2013.
doi:10.1088/1674-1137/37/6/067001

[17] H. Hotchi, "Effects of the Montague resonance on the formation of the beam distribution during multiturn injection painting in a high-intensity proton ring", *Phys. Rev. Accel. Beams,* vol. 23, p. 050401, 2020.
doi:10.1103/PhysRevAccelBeams.23.050401

[18] M.-Y. Huang, Y. Irie, S.-Y. Xu, X. Qi, and S. Wang, "Performance of the correlated painting based on the mechanical structure of the anti-correlated painting scheme", *Phys. Rev. Accel. Beams,* vol. 25, p. 110401, 2022.
doi:10.1103/PhysRevAccelBeams.25.110401

[19] H. Liu and S. Wang, "Longitudinal beam dynamic design of 500 kW beam power upgrade for CSNS-II RCS", *Radiat. Detect. Technol. Methods*, vol. 6, pp. 339–348, 2022.
doi:10.1007/s41605-022-00325-5

[20] Y. Liu, L. Huang, S. Wang, N. Wang, and Y. Li, "Impedance and beam instability in RCS/CSNS", *High Power Laser and Part. Beams*, vol. 25, no. 2, pp. 465-470, 2013 (in Chinese).
doi:10.3788/hplpb20132502.0465

[21] N. Wang, "Coupling impedance and collective effects in the RCS ring of the China Spallation Neutron Source", Ph. D. Thesis, University of Chinese Academy of Sciences, 2009 (in Chinese), http://impedance.web.cern.ch/documents/Na%20Wang.pdf

[22] IW2D, https://gitlab.cern.ch/IRIS/IW2D.git

[23] N. Mounet and E. Métral, "Electromagnetic fields and beam coupling impedances in a multilayer flat chamber", CERN, Geneva, Switzerland, Rep. No. CERN-ATS-Note-2010-056 TECH, Dec. 2010,
https://cds.cern.ch/record/1314524

[24] L. Huang, Y. Liu, and S. Wang, "Resistive wall instability in rapid Cycling synchrotron of China spallation neutron source", *Nucl. Instrum. Methods Phys. Res., Sect. A*, vol. 728, pp. 1-5, 2013.
doi:10.1016/j.nima.2013.06.017

[25] A. W. Chao, *Physics of Collective Beam Instabilities in High Energy Accelerators*, Wiley, New York, 1993.